

Three-cascaded 1407-nm Raman laser based on phosphorus-doped silica fiber

E. M. Dianov, I. A. Bufetov, M. M. Bubnov, M. V. Grekov, S. A. Vasiliev, and O. I. Medvedkov

*Fiber Optics Research Center at the General Physics Institute of the Russian Academy of Sciences,
38 Vavilov Street, Moscow 117756, Russia*

Received October 20, 1999

We report a laser-diode-pumped 1407-nm Raman fiber laser with an output power of 1 W. In this three-cascaded cw Raman laser, based on a single active phosphorus-doped silica fiber, for the first time to the authors' knowledge successive generation of Stokes components of essentially different frequency shifts (1330 and 490 cm^{-1}) has been realized. These Stokes components are associated with both constituents (P_2O_5 and SiO_2) of the fiber core glass. © 2000 Optical Society of America

OCIS codes: 060.2320, 140.3510, 140.3550, 190.4370.

Recently, remarkable progress has been made in the development of Raman fiber lasers (RFL's) pumped by Nd (or Yb) double-clad fiber lasers. Multicascaded RFL's based on GeO_2 -doped fiber permit the efficient generation of light up to a wavelength of 1.48 μm .^{1,2} The low value of the GeO_2 -related Stokes shift (440 cm^{-1}) along with the proper choice of the Nd (Yb) laser pump wavelength permits generation of radiation at practically any wavelength in the region near 1–1.5 μm . However, the low value of the GeO_2 -related Stokes shift leads to a large number of cascades in the Raman frequency conversion to the long-wavelength side of this region and correspondingly to a complicated optical scheme and decreased efficiency.

Efficient operation of a RFL based on P_2O_5 -doped silica fibers was demonstrated recently.^{3–5} The large value of the Raman shift in phosphosilicate fibers (1330 cm^{-1}) reduces the number of cascades. But the relatively narrow P_2O_5 -related Stokes band along with the large value of Raman shift in P_2O_5 -doped fibers does not enable light to be generated at all wavelengths at which generation of light may be desired.

In this Letter we report, for the first time to our knowledge, a Raman fiber laser based on a single P_2O_5 -doped silica fiber with successive generation of Stokes components associated with both constituents of the core glass (P_2O_5 and SiO_2). Such a RFL combines the advantages of the RFL's mentioned above. It can generate practically any wavelength up to 1.6 μm by using not more than three conversion cascades.

Because of the great interest in exploiting the 1450–1530-nm spectral region for optical communication, we have developed a three-cascaded 1407-nm RFL that can serve as a pump unit for the 1500-nm Raman fiber amplifier. To attain the necessary wavelength of 1407 nm we used one P_2O_5 -related and two SiO_2 -related Stokes shifts.

A single-mode P_2O_5 -doped fiber with a second-mode cutoff wavelength of 0.91 μm was chosen as the active Raman medium for the 1407-nm laser. This fiber was manufactured by the modified chemical-vapor deposition method. The difference in refractive indices of the core and the cladding was (in preform)

0.011, which corresponds to a 13 mol.% P_2O_5 doping level. The preform was sleeved with additional tubes before being drawn into a fiber.

Highly P_2O_5 -doped single-mode fibers usually demonstrate relatively high optical losses of 2–4 dB/km in the 1.1–1.5- μm spectral region.^{6–8} Decreasing the drawing temperature and codoping the phosphosilicate core with fluorine permit reduction of optical losses in highly P_2O_5 -doped fibers.⁹ Figure 1 shows the spectral attenuation curve for the fiber produced by this method.

The working wavelength (1407 nm) of our Raman laser is in the region of the absorption peak that is due to the first overtone of the Si–OH fundamental absorption band at 2.74 μm . However, the OH formation mechanism in the P_2O_5 -doped fibers is different from that in GeO_2 -doped fibers. It has been shown¹⁰ that hydroxyl radicals can be trapped at phosphorus sites in P_2O_5 -doped silica, resulting in the shift of the fundamental Si–OH absorption at 2.74 to 3.05 μm . The first overtone of this absorption reveals itself as broad absorption in the vicinity of 1.6 μm . A small absorption peak near 1.4 μm that appears in the spectral attenuation curve of the single-mode fiber seems to be

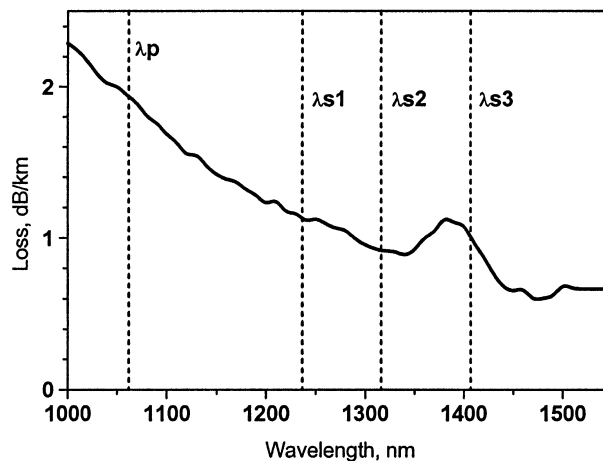


Fig. 1. Optical loss spectrum of a P-doped fiber. λ_p , λ_{s1} , λ_{s2} , λ_{s3} , wavelengths of pump radiation and its successive Stokes components.

due to partial penetration of the mode field into the substrate tube. This peak is not observed in the spectral attenuation curve of multimode fiber drawn from the same preform.

One of the most important parameters of the Raman laser active medium is the Raman gain coefficient. The fiber Raman gain coefficient (FRGC) of the chosen P-doped fiber was measured at the wavelengths of P_2O_5 - and SiO_2 -related Stokes bands. The FRGC at the wavelength $1.24 \mu m$, with the pump at $1.06 \mu m$ (P_2O_5 -associated Stokes), was $g_0(1.24/1.06) = 6.8 \text{ dB}/(\text{km W})$. The values of $g_0(1.24/1.06)$ for several other P-doped fibers manufactured by the same technology, but with different values Δn , also were measured (see Fig. 2, open triangles). These values were measured through the generation threshold of the Raman laser with the well-known losses in the cavity (the experiment is described in Ref. 11). The SiO_2 -related FRGC (Stokes shift of 440 cm^{-1}) was measured in a $1.3\text{-}\mu m$ Raman optical amplifier with a pump wavelength of $1.24 \mu m$, as it was made with highly GeO_2 -doped fiber.¹² The value of the FRGC was $g_0(1.3/1.24) = 5.4 \text{ dB}/(\text{km W})$.

Note that the FRGC for the P-doped fiber can be estimated by use of the well-known values of the Raman gain coefficient for the bulk silica¹³ and the relative Raman cross section of vitreous P_2O_5 .¹⁴ We calculated the values of $g_0(1.24/1.06)$ and $g_0(1.3/1.24)$ by making the following assumptions: (1) The index difference Δn between the P_2O_5 -doped silica core and the silica cladding is due only to the addition of P_2O_5 , and the value of Δn is proportional to the P_2O_5 concentration. (2) The Raman gain coefficient of the bulk core material is proportional to the P_2O_5 concentration, and its maximum value corresponds to that indicated in Ref. 14. The relative Raman cross section of P_2O_5 (Raman shift, $\sim 1330 \text{ cm}^{-1}$) is 3.5 times higher than that for pure silica at 440 cm^{-1} . (3) The mode field distributions for the signal and for the pump radiation were calculated with the real Δn profile in the preform taken into account. The real value of Δn in the fiber is $\sim 10\%$ less than in the preform because of the diffusion of P_2O_5 during the fiber drawing.

The results of the calculation are shown in curves 1 and 2 of Fig. 2, along with the experimental results. The value of the calculated FRGC at the SiO_2 -related Stokes wavelength is in good agreement with the measured value. But there is a considerable discrepancy between the measured and the calculated values of $g_0(1.24/1.06)$. Our experimental results show that the relative Raman cross section for P_2O_5 (at the 1330-cm^{-1} band) in silica is approximately 2.6 times greater than that given in Ref. 14 for melted pure P_2O_5 . This fact is also in accordance with the analysis of the generation processes in Raman lasers^{3-5,11} (because these lasers would not be able to operate at such a low FRGC, as indicated by curve 2 of Fig. 2) and with the analysis of the Raman spectrum of the phosphosilicate fiber³ (the amplitude of the 1330-cm^{-1} peak in the Raman spectrum of phosphosilicate fiber with $\sim 13 \text{ mol. \% } P_2O_5$ is higher than that of the 490-cm^{-1} SiO_2 -related peak). It is no wonder that the Raman cross section of P_2O_5 (at the 1330-cm^{-1} band) has

different values for samples of different compositions (as was shown in Ref. 14) and prepared by different technologies. The discrepancy observed can be associated with different relative concentrations of double bonds $P=O$ (responsible for the 1330-cm^{-1} Raman band) in P_2O_5 -doped silica fiber and in a fused vitreous pure P_2O_5 bulk sample. The properly corrected calculated data for the P_2O_5 -associated FRGC are shown in curve 3 of Fig. 2.

A schematic of the 1407-nm Raman fiber is shown in Fig. 3. The setup includes the laser diode array (LDA) pump module (Opto Power OPC-D010-805-HB/250), a Nd-doped double-clad fiber laser, and a three-cascaded Raman converter. Bragg gratings, written in short pieces of standard fiber (Flexcor 1060), form all the optical cavities. The laser-diode array multimode pump radiation ($\lambda = 0.805 \mu m$) was transformed into cw single-mode radiation of the Nd fiber laser with wavelength $\lambda_p = 1.062 \mu m$. The maximum output power of the Nd laser was 3.8 W .

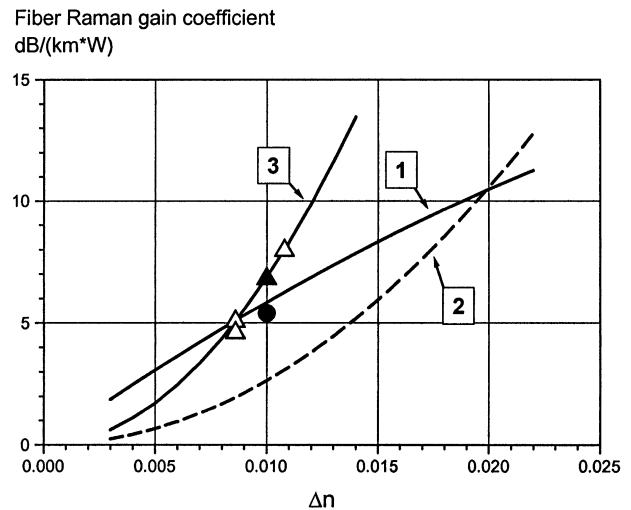


Fig. 2. Variation of the fiber Raman gain coefficients with Δn in the fiber. 1: $g_0(1.31/1.24)$, calculated; filled circles, experiment. 2: $g_0(1.24/1.06)$, calculated; triangles, experiment. Filled symbols refer to the P-doped fiber used as the Raman medium for a 1407-nm laser. 3: $g_0(1.24/1.06)$, corrected.

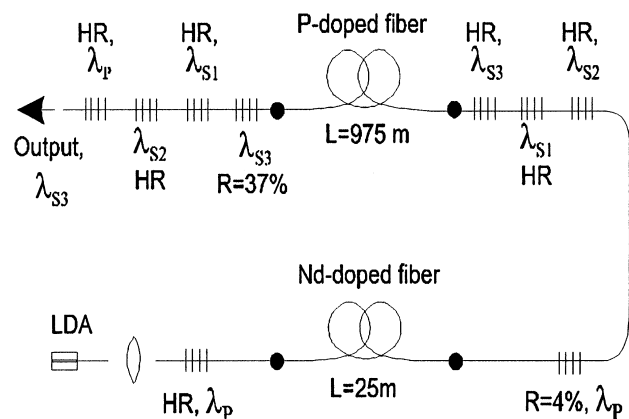


Fig. 3. Schematic of the 1407-nm P-doped silica-fiber-based Raman laser: HR, highly reflecting; R , reflection; L , length.

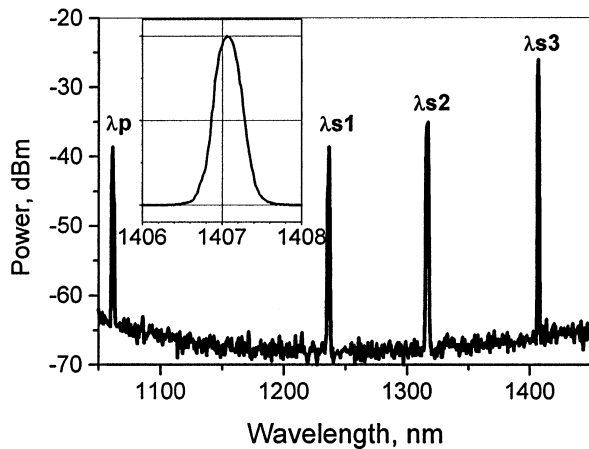


Fig. 4. Spectrum of the RFL output radiation. Inset, the 1407-nm band.

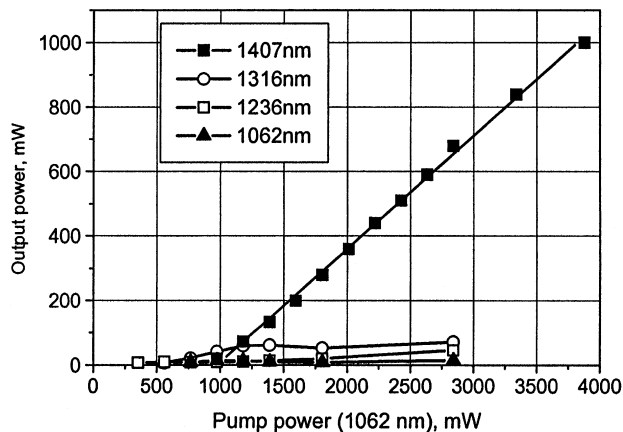


Fig. 5. Output power of the Raman laser versus the pump power of the Nd fiber laser.

The length of the P-doped silica fiber was 975 m. It is important that the active fiber had relatively low optical losses i.e., 1.1 dB/km at 1.407 μm (Fig. 1). The close values of the SiO_2 - and P_2O_5 -associated Raman gain coefficients enabled us to use the generation of both SiO_2 - and P_2O_5 -related Stokes components simultaneously.

The RFL had three embedded optical cavities at wavelengths $\lambda_{s1} = 1236$ nm, $\lambda_{s2} = 1316$ nm, and $\lambda_{s3} = 1407$ nm, three successive Stokes wavelengths. λ_{s1} corresponds to the P-associated Stokes shift of 1330 cm^{-1} ; λ_{s2} and λ_{s3} , to the SiO_2 -associated Stokes shift of 490 cm^{-1} . So, to attain the necessary wavelength of 1407 nm in an efficient cascade RFL based on a single P-doped silica fiber, we used successive generation of Stokes components associated with different constituents of the fiber core (P_2O_5 and SiO_2).

The output spectrum of the Raman laser is shown in Fig. 4. The dependence of the output power at λ_{s3} on the pump power at λ_p is shown by filled squares in Fig. 5. A laser slope efficiency of 35% was observed. This value may be considered high enough when the sharp dependence of the RFL efficiency on the loss level in the Raman laser cavity is taken into account.¹¹ Open circles, open squares, and filled triangles in Fig. 5 illustrate the output power at wavelengths λ_{s2} , λ_{s1} , and λ_p , respectively.

In conclusion, we have demonstrated the possibility of use of a P-doped silica fiber as an efficient Raman gain medium in a wide wavelength range. A three-cascaded 1407-nm Raman laser was developed with an output power of 1 W. A Raman laser slope efficiency of 35% was achieved. Raman fiber lasers based on P-doped fibers can serve as pump sources for Raman amplifiers at any wavelength in the region 1.1–1.6 μm .

References

1. S. G. Grubb, T. Erdogan, V. Mizrahi, T. Strasser, W. Y. Cheung, W. A. Reed, P. J. Lemaire, A. E. Miller, S. G. Kosinski, G. Nykolak, P. C. Becker, and D. W. Peckham, in *Optical Amplifiers and Their Applications*, Vol. 14 of 1994 OSA Technical Digest Series (Optical Society of America, Washington, D.C., 1994), paper PD3.
2. S. G. Grubb, T. Strasser, W. Y. Cheung, W. A. Reed, V. Mizrahi, T. Erdogan, P. J. Lemaire, A. M. Vengsarkar, D. J. DiGiovanni, D. W. Peckham, and B. H. Rockney, in *Optical Amplifiers and Their Applications*, Vol. 5 of OSA Trends in Optics and Photonics Series (Optical Society of America, Washington, D.C., 1995), paper S.S4.
3. E. M. Dianov, M. V. Grekov, I. A. Bufetov, S. A. Vasiliev, O. I. Medvedkov, V. G. Plotnichenko, V. V. Koltashev, A. V. Belov, M. M. Bubnov, S. L. Semjonov, and A. M. Prokhorov, *Electron. Lett.* **33**, 1542 (1997).
4. E. M. Dianov, I. A. Bufetov, M. M. Bubnov, A. V. Shubin, S. A. Vasiliev, O. I. Medvedkov, S. L. Semjonov, M. V. Grekov, V. M. Paramonov, A. N. Gur'yanov, V. F. Khopin, D. Varelal, A. Iocco, D. Costantini, H. G. Limberger, and R.-P. Salathé, in *Optical Fiber Communication Conference (OFC)* (Optical Society of America, Washington, D.C., 1999), paper PD25.
5. V. I. Karpov, E. M. Dianov, V. M. Paramonov, O. I. Medvedkov, M. M. Bubnov, S. L. Semyonov, S. A. Vasiliev, V. N. Protopopov, O. N. Egorova, V. F. Hopin, A. N. Gur'yanov, M. P. Bachynski, and W. R. L. Clements, *Opt. Lett.* **24**, 887 (1999).
6. V. A. Aksjonov, E. N. Bazarov, A. V. Belov, E. M. Dianov, G. A. Ivanov, B. A. Isaev, V. V. Koltashev, A. A. Makovetskij, K. M. Nametov, V. G. Plotnichenko, and Ju. K. Chamorovskij, *Inorg. Mater.* **34**, 1218 (1998; in Russian).
7. A. S. L. Gomes, V. L. DaSilva, J. R. Taylor, B. G. Anslie, and S. P. Craig, *Opt. Commun.* **64**, 373 (1987).
8. K. Suzuki, K. Noguchi, and N. Uesugi, *Opt. Lett.* **11**, 656 (1986).
9. E. M. Dianov, I. A. Bufetov, V. I. Karpov, M. M. Bubnov, A. N. Gur'yanov, and V. F. Khopin, in *Optical Networking*, A. Bononi, ed. (Springer-Verlag, London, 1999), p. 165.
10. Y. Mita, S. Matsushita, T. Vanase, and H. Nomura, *Electron. Lett.* **13**, 55 (1977).
11. E. M. Dianov, I. A. Bufetov, M. M. Bubnov, M. V. Grekov, A. V. Shubin, S. A. Vasiliev, O. I. Medvedkov, S. L. Semjonov, A. N. Gur'yanov, and V. F. Khopin, presented at the 25th European Conference on Optical Communication, Nice, France, September 26–30, 1999.
12. E. M. Dianov, M. V. Grekov, I. A. Bufetov, V. M. Mashinsky, O. D. Sazhin, A. M. Prokhorov, G. G. Devyatykh, A. N. Guryanov, and V. F. Khopin, *Electron. Lett.* **34**, 669 (1998).
13. R. H. Stolen, *Proc. IEEE* **68**, 1232 (1980).
14. F. L. Galeener, J. C. Mikkelsen, Jr., R. H. Geils, and W. J. Mosby, *Appl. Phys. Lett.* **32**, 34 (1978).